

# Ultra high energy cosmic rays: implications of Auger data for source spectra and chemical composition

R. Aloisio<sup>1,2</sup>, V. Berezhinsky<sup>2,3</sup> and P. Blasi<sup>1,2</sup>

<sup>1</sup>INAF/Osservatorio Astrofisico di Arcetri, Largo E. Fermi, 5 - 50125 Firenze, Italy

<sup>2</sup>Gran Sasso Science Institute (INFN), viale F. Crispi 7, 67100 L'Aquila, Italy

<sup>3</sup>INFN/Laboratori Nazionali Gran Sasso, ss 17bis km 18+910, 67100 Assergi, Italy

E-mail: [aloisio@arcetri.astro.it](mailto:aloisio@arcetri.astro.it), [berezhinsky@lngs.infn.it](mailto:berezhinsky@lngs.infn.it), [blasi@arcetri.astro.it](mailto:blasi@arcetri.astro.it)

**Abstract.** We use a kinetic-equation approach to describe the propagation of ultra high energy cosmic ray protons and nuclei and calculate the expected spectra and mass composition at the Earth for different assumptions on the source injection spectra and chemical abundances. When compared with the spectrum, the elongation rate  $X_{max}(E)$  and dispersion  $\sigma(X_{max})$  as observed with the Pierre Auger Observatory, several important consequences can be drawn: a) the injection spectra of nuclei must be very hard,  $\sim E^{-\gamma}$  with  $\gamma \sim 1 - 1.6$ ; b) the maximum energy of nuclei of charge  $Z$  in the sources must be  $\sim 5Z \times 10^{18}$  eV, thereby not requiring acceleration to extremely high energies; c) the fit to the Auger spectrum can be obtained only at the price of adding an *ad hoc* light extragalactic component with a steep injection spectrum ( $\sim E^{-2.7}$ ). In this sense, at the ankle ( $E_A \approx 5 \times 10^{18}$  eV) all the components are of extragalactic origin, thereby suggesting that the transition from Galactic to extragalactic cosmic rays occurs below the ankle. Interestingly, the additional light extragalactic component postulated above compares well, in terms of spectrum and normalization, with the one recently measured by KASCADE-Grande.

---

## Contents

<b>1</b>	<b>Introduction</b>	<b>1</b>
<b>2</b>	<b>Spectra of UHECRs propagating through the CMB and EBL</b>	<b>3</b>
<b>3</b>	<b>Building models: problems and progress</b>	<b>7</b>
3.1	Galactic EeV component	9
3.2	Extragalactic EeV component and KASCADE-Grande light component	11
<b>4</b>	<b>Discussion and conclusions</b>	<b>13</b>

---

## 1 Introduction

One century after the discovery of Cosmic Rays (CR) a general description of the basic aspects of the problem has been achieved but numerous crucial pieces of the puzzle still fail to fall in place. In the energy range that spans from few GeV/n up to  $10^3$  TeV/n a self consistent scenario that accommodates CR composition, propagation and sources has been developed in the last 30 years, the so-called standard model of galactic CR (for reviews see [1, 2] and references therein).

Most CRs with energies below the knee are believed to be produced in Galactic sources, while their propagation time inside the Galaxy is energy dependent. The knee reflects a change in the chemical composition from light to heavy and is well described as a result of rigidity dependent acceleration and propagation of CRs with gradually larger mass. The observed CR flux requires a total power of few percent of the energy released in a supernova (SN) explosion. This fact is at the very base of Diffusive Shock Acceleration (DSA) models, that describe CR acceleration in terms of collisionless interactions of particles with shocks driven by the expanding shell of a supernova remnant (SNR) [3, 4, 5].

The basic version of the SNR paradigm leads to expect that Galactic CRs should extend to energies of the order of a few  $10^{17}$  eV and that at such energies the chemical composition should be dominated by iron nuclei. This should be the end of the Galactic CR spectrum.

The origin of ultra high energy CRs (UHECRs) is still enshrouded in mystery: their sources are unknown, their chemical composition is subject of much debate and their same definition is somewhat tricky since it is directly related to the end of Galactic CRs. The propagation of UHECRs (protons, nuclei and photons) on cosmological distances has been investigated in detail by many authors and the underlying physics is well known. The main source of uncertainty in this problem consists in a poor knowledge of the intergalactic magnetic fields (if present at all) and the cosmic evolution of the extragalactic background light (EBL). While the cosmological evolution of the CMB is known, the evolution with redshift of the EBL should be inferred from observations at different redshifts through the use of specific models [6, 7]. These models are in good agreement at low redshift ( $z < 4$ ), most relevant for the propagation of UHECR nuclei, while showing significant differences at high redshift ( $z > 4$ ), thereby affecting the production of cosmogenic neutrinos (see [8] and references therein). Here we use the results of [6] to model the EBL radiation field and its cosmological evolution.

The propagation of UHE nucleons<sup>1</sup> is affected only by the interaction with the CMB radiation field [9, 10] and leads to the appearance of two spectral features: the pair-production dip [11, 12], which is a rather faint feature caused by the pair production process ( $p + \gamma_{CMB} \rightarrow e^+ + e^- + p$ ), and a sharp steepening of the spectrum caused by pion photo-production ( $p + \gamma_{CMB} \rightarrow \pi + p$ ) called Greisen-Zatsepin-Kuzmin (GZK) cutoff [13, 14]. The position of the GZK feature is roughly defined by the energy where the pair-production and the photo-pion production rates of energy loss become equal, namely at  $E_{eq} = 6.05 \times 10^{19}$  eV [11], which approximately corresponds to  $E_{GZK} \simeq 50$  EeV

The propagation of UHE nuclei is affected by pair production and photo-disintegration on the CMB and in general on the EBL. In the latter process a nucleus with atomic mass number  $A$  loses one or more nucleons because of its interaction with the CMB and the EBL,  $A + \gamma_{CMB,EBL} \rightarrow (A - nN) + nN$ , being  $n$  the number of nucleons lost by the nucleus [9, 10]. The photo-disintegration of nuclei leads to a steepening in the observed spectrum compared with the injection spectrum. The interplay between these processes has important consequences in terms of chemical composition of UHECRs, as discussed below.

From the experimental point of view, measurements of the spectrum and chemical composition of UHECRs appear to be still not conclusive: HiRes and Telescope Array (TA) claim that the chemical composition is compatible with being proton-dominated up to the highest energies.

A somewhat different picture arises from observations carried out with the Pierre Auger observatory: the published data at the time of writing of this paper show that the spectrum is not directly understood in terms of a pure proton composition. The elongation rate and its dispersion, when used to infer the chemical composition of UHECRs, clearly suggest that a gradual transition from light to heavy composition takes place between  $10^{18}$  eV and  $\sim 5 \times 10^{19}$  eV [15]<sup>2</sup>.

The qualitatively new finding that the mass composition of UHECRs might be mixed has served as a stimulus to finding propagation models that can potentially explain the phenomenology of Auger data. Here we investigate these models and try to address the complex issue of the transition from Galactic to extragalactic cosmic rays. We show that the Auger spectrum and mass composition at  $E \geq 5 \times 10^{18}$  eV can be fitted at the same time only at the price of requiring very hard injection spectra for all nuclei ( $\sim E^{-\gamma}$  with  $\gamma = 1 - 1.6$ ) and a maximum rigidity of  $\sim 5Z \times 10^{18}V$ . One should appreciate the change of paradigm that this finding implies: while a decade ago the focus of this field of research was to find sources and acceleration mechanisms able to energize CR protons up to energies in excess of  $\sim 10^{20}$  eV, present data require that the UHECR part of the spectrum is made of heavy nuclei and that protons' maximum energy should not exceed a few  $EeV$ . Moreover, rather unusual sources are being implied, in that the injection spectra are at odds with the predictions of standard acceleration mechanisms.

However, by accepting these conclusions, it follows that the spectrum of Auger at energies below 5 EeV requires an additional component and we show that it has to be made of

---

<sup>1</sup>Hereafter we will only consider protons because, as discussed in [8, 9, 10], the decay time of neutrons is much shorter than all other time scales involved in the propagation of UHE particles.

<sup>2</sup>A recalibration of the Auger energy scale is being carried out. Preliminary data presented at the 33<sup>rd</sup> International Cosmic Ray Conference show a better agreement with the HiRes and TA spectra at low energies, while a difference in the GZK region remains. Elongation rate and dispersion are also affected by the correction in the energy scale but the qualitative picture is not significantly affected by these new results. The differences between the two experiments in terms of mass composition were recently investigated in a critical way by a working group made of members of the Auger, TA and Yakutsk collaborations [16].

light nuclei (protons and helium nuclei) of extragalactic origin. This implies that at the ankle all particles are of extragalactic origin, so that the transition from galactic to extragalactic CRs must occur at somewhat lower energies.

In the energy region  $10^{17} - 10^{18}$  eV the newly released data of the KASCADE-Grande (KG) collaboration [17, 18] and of the IceTop collaboration [19]) may help clarifying the situation. In Refs. [17, 18, 20] the presence of two separate CR components is discussed: one light (mainly protons and helium) and the other heavy (mainly iron) with different spectra. The results of IceTop [19] appear to be in qualitative agreement with those of KG. At  $10^{18}$  eV the flux of light and heavy nuclei appear to have comparable fluxes, in marginal friction with the results of the three largest UHECR detectors, HiRes, TA and Auger, that are all compatible with a proton-dominated composition at EeV energies. This friction should however be taken with much caution since the absolute fluxes of CRs with different masses as measured by KG are strongly dependent upon the adopted model of interactions in the atmosphere, as recently discussed in [21].

It is however interesting to notice that the light component of KG fits well in terms of spectrum and absolute flux the one that we require as additional extragalactic component discussed above and solely based on fitting the Auger data.

To model the propagation of UHECR we refer to the theoretical framework based on kinetic equations with a homogeneous distribution of sources [9, 10]. The paper is organized as follows: in §2 we introduce the basic theoretical tools and assumptions used in our calculations, in §3 we focus on the Auger data and discuss the minimal requirements needed to achieve a description of the flux and chemical composition. We also comment on the implications of these models for the transition from Galactic to extragalactic CRs and compare our results with the recent data of KASCADE-Grande. We conclude in §4.

## 2 Spectra of UHECRs propagating through the CMB and EBL

In this section we briefly summarize the technical aspects of the calculations carried out below, and we provide references to relevant work in which more details can be found.

While propagating through the CMB and the EBL, UHE protons and nuclei undergo energy losses due to the following processes: expansion of the universe (adiabatic energy losses), production of  $e^+ + e^-$  pairs, pion production (for protons) and photo-disintegration (for nuclei). These processes are treated here in the context of the continuous energy-loss (CEL) approximation, which *a priori* is not justified for  $p + \gamma \rightarrow N + \pi$ . However, as demonstrated in [11], in the case of a homogeneous distribution of sources, the fluctuations in the kinetic equation formalism give a negligible effect up to energy  $10^{21} - 10^{22}$  eV. This is also true for photo-disintegration of nuclei, as demonstrated by the good agreement [10] between the kinetic calculations and different MC schemes [22, 23, 24]. However, the role of fluctuations can become important in the case of a discrete distribution of sources when the mean distance between sources is comparable (or larger) with the interaction length of particles.

The process of photo-disintegration leaves the Lorentz factor of the nucleus unaltered, and the process can be considered as a *decay*. The lifetime of a nucleus of atomic mass number  $A$  and Lorentz factor  $\Gamma$  at the cosmological time  $t$  depends on both the CMB and EBL background fields and can be written as

$$\frac{1}{\tau_A(\Gamma, t)} = \frac{c}{2\Gamma^2} \int_{\epsilon_0(A)}^{\infty} d\epsilon_r \sigma(\epsilon_r, A) \nu(\epsilon_r) \epsilon_r \int_{\epsilon_r/(2\Gamma)}^{\infty} d\epsilon n(\epsilon, t) / \epsilon^2, \quad (2.1)$$

where  $\epsilon$  is the energy of the target (background) photon in the laboratory frame and  $\epsilon_r$  is the same energy in the rest frame of the nucleus,  $\epsilon_0(A)$  is the threshold of the considered reaction in the rest frame,  $n(\epsilon, t)$  is the density of the background photons at the cosmological time  $t$ , given by  $n(\epsilon, t) = n_{\text{CMB}} + n_{\text{EBL}}$  and  $\sigma(\epsilon_r, A)$  is the cross-section of photo-disintegration. For the EBL we use the cosmological evolution model of Ref. [6].

In principle the photo-disintegration process involves the emission of one or more nucleons as described by the multiplicity  $\nu(\epsilon)$  in equation (2.1). As discussed in [9, 25, 26], the dominant photo-disintegration channel is the one leading to the emission of one nucleon ( $\nu = 1$ ) that corresponds to the giant dipole resonance in the photo-disintegration cross section. In [9, 10] multinucleon emission ( $\nu > 1$ ) was included and found to be rather small. In this paper we only include the channel with  $\nu = 1$ .

At large Lorentz factors, photo-disintegration occurs on low energy CMB photons and the corresponding lifetime of the nucleus  $\tau_A(\Gamma)$  is short, while at small Lorentz factors the lifetime is dominated by the EBL and  $\tau_A(\Gamma)$  is large. The critical Lorentz factor  $\Gamma_c$  where the transition between the two regimes occurs is determined by the equality

$$\tau_A^{\text{EBL}}(\Gamma_c) = \tau_A^{\text{CMB}}(\Gamma_c). \quad (2.2)$$

For  $\Gamma > \Gamma_c$  the lifetime sharply decreases and the spectrum of nuclei becomes steeper, which can be referred to as photo-disintegration cutoff or Gerasimova-Rozental (GR) cutoff (see [27]).

**Table 1.** Critical Lorentz factor  $\Gamma_c$  and photo-disintegration cutoff  $E_{\text{GR}}$ .

nuclei	He <sup>4</sup>	N <sup>14</sup>	Mg <sup>24</sup>	Ca <sup>40</sup>	Fe <sup>56</sup>
$\Gamma_c$	$5 \times 10^9$	$4 \times 10^9$	$3.5 \times 10^9$	$4 \times 10^9$	$3.2 \times 10^9$
$E_{\text{GR}}$	$2.0 \times 10^{19}$	$5.6 \times 10^{19}$	$8.4 \times 10^{19}$	$1.6 \times 10^{20}$	$1.8 \times 10^{20}$

The corresponding critical Lorentz factor  $\Gamma_c$  and photo-disintegration cutoff  $E_{\text{GR}} = \Gamma_c A m_N$  are shown in Table 1 for selected nuclei. The critical Lorentz factor is approximately the same for all nuclei of interest,  $\Gamma_c \approx 4 \times 10^9$ , with the largest one for He<sup>4</sup> ( $\Gamma_c = 5 \times 10^9$ ) and an anomalously low one for Be<sup>9</sup> ( $6 \times 10^8$ ) and the next lowest  $\Gamma_c = 3.2 \times 10^9$  for iron. The constancy of  $\Gamma_c$  is easily understood based on the relation  $\Gamma_c \epsilon_t \sim \epsilon_0$ , where  $\epsilon_t$  is the typical energy of a target photon and  $\epsilon_0$  is the binding energy of the nucleus.

In Tabel 1 the critical Lorentz factors  $\Gamma_c$  and photo-disintegration cutoffs  $E_{\text{GR}} = A\Gamma_c m_N$  are listed for various nuclei. The approximate independence of  $\Gamma_c$  on the type of nucleus has profound implications for the high energy end of the fluxes of nuclei. Together with  $E_{\text{GR}} = A\Gamma_c m_N$ , the second energy scale that fixes the flux behavior at the highest energies is the maximum acceleration energy  $E_A^{\text{max}} = Z E_p^{\text{max}} = Z m_N \Gamma_p^{\text{max}}$ , an intrinsic characteristic of the acceleration process, that hereafter we assume to be rigidity dependent, namely proportional to the charge  $Z$  of the accelerated nucleus.

The photo-disintegration cutoff in the observed spectrum appears if  $E_{\text{GR}} < E_A^{\text{max}}$ . In the opposite case,  $E_{\text{GR}} > E_A^{\text{max}}$ , the high energy end of the spectra is not due to photo-disintegration, because of the lack of particles with  $E_A > E_A^{\text{max}}$ , and the flux suppression is due to the acceleration cutoff  $E_A^{\text{max}} = Z \Gamma_p^{\text{max}} m_N$ . If one assumes for simplicity that  $A \approx 2Z$

and  $\Gamma_c \simeq 4 \times 10^9$ , the condition  $E_{GR} > E_{max}^A$  becomes:

$$\Gamma_{max}^p < \frac{A}{Z} \Gamma_c \sim 8 \times 10^9.$$

In this regime, dominated by the maximum acceleration energy, the photo-disintegration manifests itself as a slow process on the EBL radiation. This process does not change the Lorentz-factor of nuclei, which is affected only by the pair production on the CMB radiation that is even slower than the photo-disintegration on EBL.

The spectra of nuclei at Earth are calculated by solving analytically the kinetic transport equations for primary and secondary nuclei and nucleons. For protons  $p$  and nuclei with mass number  $A$  these equations read:

$$\frac{\partial n_p(\Gamma, t)}{\partial t} - \frac{\partial}{\partial \Gamma} [b_p(\Gamma, t)n_p(\Gamma, t)] = Q_p(\Gamma, t) \quad (2.3)$$

$$\frac{\partial n_A(\Gamma, t)}{\partial t} - \frac{\partial}{\partial \Gamma} [n_A(\Gamma, t)b_A(\Gamma, t)] + \frac{n_A(\Gamma, t)}{\tau_A(\Gamma, t)} = Q_A(\Gamma, t) \quad (2.4)$$

where  $n$  is the equilibrium distribution of particles,  $b = -d\Gamma/dt$  is the rate of decrease of the particle Lorentz factor, and  $Q_p$  and  $Q_A$  are the production rates per unit co-moving volume and time of protons and nuclei, as the sum of those produced inside the sources and the secondary products of photo-disintegration. Particles are assumed to be accelerated at unspecified, homogeneously distributed sources in a rigidity dependent manner.

For the primary particles we consider three cases of injection/acceleration. For reasons that will become clear later, we are especially interested in the case of hard injection, where the slope of the generation spectrum is  $\gamma_g < 2.0$ . When normalized to the energy injected per unit comoving volume and time  $\mathcal{L}_0$ , the CR spectrum reads:

$$Q_{A_0}^{\text{acc}}(\Gamma) = \frac{(2 - \gamma_g)\mathcal{L}_0}{A_0 m_N} \frac{1}{\Gamma_0^2} \left( \frac{\Gamma}{\Gamma_0} \right)^{-\gamma_g} e^{-\Gamma/\Gamma_{max}}, \quad (2.5)$$

with  $A_0 = 1$  in the case of protons. In the special case  $\gamma_g = 1$  one has:

$$Q_{A_0}^{\text{acc}}(\Gamma) = \frac{\mathcal{L}_0}{A m_N \Gamma_0} \frac{1}{\Gamma} e^{-\Gamma/\Gamma_{max}}. \quad (2.6)$$

The spectrum of CRs effectively injected in the intergalactic medium by a collection of sources can be affected by the convolution of the spectrum of individual sources and their luminosity and/or maximum energy achieved. For instance, under realistic assumptions [28] the spectra of protons and primary nuclei can have a broken power-law spectrum. In [12] a correlation between the source luminosity and the maximum achievable energy was used to derive an effective injection spectrum with the following shape:

$$Q_{A_0}^{\text{acc}}(\Gamma) = \frac{\mathcal{L}_0/(A_0 m_N)}{\ln \Gamma_0 + 1/(\gamma_g - 2)} q_{\text{gen}}(\Gamma) e^{-\Gamma/\Gamma_{max}}, \quad (2.7)$$

with

$$q_{\text{gen}}(\Gamma) = \begin{cases} 1/\Gamma^2 & \text{at } \Gamma \leq \Gamma_0 \\ \frac{1}{\Gamma_0^2} \left( \frac{\Gamma}{\Gamma_0} \right)^{-\gamma_g} & \text{at } \Gamma \geq \Gamma_0. \end{cases} \quad (2.8)$$

Here the low energy slope  $\sim 2$  was inspired by the traditional diffusive shock acceleration canonical result, while the slope  $\gamma_g > 2$  for Lorentz factor  $\Gamma > \Gamma_0$  might be due to convolution

of  $\sim E^{-2}$  spectra with different cutoffs from sources with different luminosities (see for instance [12, 28]). The value of  $\Gamma_0$  in (2.5), (2.6) and (2.7) depends on the specific adopted model, but for phenomenological purposes one has to assume  $\Gamma_0 \sim 10^6 - 10^8$ , as it makes the requirements in terms of  $\mathcal{L}_0$  less severe.

After acceleration in the sources, nuclei with mass number  $A_0$  propagate in the intergalactic medium where they can suffer photo-disintegration, which leads to injection of secondary nuclei with  $A < A_0$  and secondary protons. As discussed above, the main channel of photo-disintegration is the extraction of one nucleon  $(A + 1) + \gamma \rightarrow A + N$ . The primary nucleus, the secondary nucleus and the associated nucleon all have approximately the same Lorentz factor  $\Gamma$ , therefore the injection rate of secondary particles can be written as:

$$Q_A^{\text{sec}}(\Gamma, z) = Q_p^{\text{sec}}(\Gamma, z) = \frac{n_{A+1}(\Gamma, z)}{\tau_{A+1}(\Gamma, z)}. \quad (2.9)$$

Equation (2.9) couples together the transport equations for nuclei, Eqs. (2.4), that should be solved following the photo-disintegration chain, namely starting from the solution for the primary injected nucleus with mass number  $A_0$  and then using the solution to solve the equation for the nuclei with mass number  $A_0 - 1$ , moving downward along the photo-disintegration chain till the lowest mass secondary nucleus  $A = 2$  is reached. The equilibrium distribution for protons  $n_p$  is obtained by solving Eq. (2.3) with both the injection of freshly accelerated protons and secondary protons produced by the photo-disintegration of nuclei taken into account:

$$Q_p = Q_p^{\text{acc}} + \sum_{A < A_0} Q_p^{\text{sec}}.$$

We complete the discussion above by presenting the analytical solution to equations (2.3) and (2.4), written as a function of redshift  $z$  and particles' Lorentz factor  $\Gamma$ . Following [9, 10] the solution reads:

$$n_p(\Gamma, z) = \int_z^{z_{\text{max}}} \frac{dz'}{(1+z')H(z')} Q_p(\Gamma', z') \left( \frac{d\Gamma'}{d\Gamma} \right)_p, \quad (2.10)$$

$$n_A(\Gamma, z) = \int_z^{z_{\text{max}}} \frac{dz'}{(1+z')H(z')} Q_A(\Gamma', z') \left( \frac{d\Gamma'}{d\Gamma} \right)_A e^{-\eta_A(\Gamma', z')}, \quad (2.11)$$

where  $d\Gamma'/d\Gamma$  for protons and nuclei was calculated in [9, 10, 29] and the generation functions  $Q_p$  and  $Q_A$  for primary and secondary particles are described by equations (2.5), (2.6) and (2.9). The term  $e^{-\eta_A}$  in equation (2.11) takes into account the effect of photo-disintegration of the propagating nucleus  $A$  and suppresses the flux as from our hypothesis of photo-disintegration behaving as a "decay" process:

$$\eta_A(\Gamma', z') = \int_z^{z'} \frac{dz''}{(1+z'')H(z'')} \frac{1}{\tau_A(\Gamma'', z'')}. \quad (2.12)$$

We conclude this section summarizing the main parameters and relevant energy scales of the physics involved in our investigation. The hypothesis of homogeneously distributed sources with power law injection fixes the source parameters: emissivity  $\mathcal{L}_0$ , injection power law index  $\gamma_g$  and maximum acceleration energy, assumed to be rigidity dependent,  $E_A^{\text{max}} = ZE_{\text{max}}^p = Zm_N\Gamma_{\text{max}}^p$ . The most relevant energy scale in the physics of propagation of UHE

nuclei is the photo-disintegration cut-off  $E_{GR} = Am_N\Gamma_c$ . As discussed above, this energy scale affects the high energy end of the flux of UHE nuclei only in the case of large enough maximum acceleration energy:  $\Gamma_{\max}^p > (A/Z)\Gamma_c$ .

### 3 Building models: problems and progress

In this section we build models aimed at describing Auger data on spectrum and chemical composition of UHECRs. In this context we adopt a phenomenological approach in which the basic source parameters ( $\gamma_g$ ,  $E_{\max}^p$  and  $\mathcal{L}_0$ ) and the relative abundances of different elements are fitted to Auger data (both spectrum and mass composition) with as little as possible *a priori* theoretical prejudice on what the values of these parameters should be.

The chemical composition is inferred from the mean value of the depth of shower maximum  $\langle X_{\max} \rangle$  and its dispersion (RMS)  $\sigma(X_{\max})$ . As was first discussed in [30] (see also [31]), the combined analysis of  $\langle X_{\max} \rangle$  and  $\sigma(X_{\max})$  allows one to obtain less model dependent information on the mass composition of UHECRs. The main uncertainties in such a procedure are introduced by the dependence of  $\langle X_{\max} \rangle$  and its fluctuations on the interaction models used to describe the shower development. Most of such models fit low energy accelerator data while providing somewhat different results when extrapolated to the energies of relevance for UHECRs (for a review see [32] and references therein).

In our calculations we follow the procedure of Ref. [33] where four models of HE interaction were included to describe the atmospheric shower development, namely EPOS 1.99 [34], Sibyll 2.1 [35], QGSJet 01 [36] and QGSJet 02 [37], in order to derive for each given primary a simple prescription for  $\langle X_{\max} \rangle$  and  $\sigma(X_{\max})$ . The Auger data are taken from Refs. [15, 38, 39]. Shadowed areas are used to illustrate the uncertainties associated with different models of shower development in the UHE regime. We stress that below we will derive only general, most essential, conclusions on different models, not trying to obtain a detailed formal fit to the Auger data.

As primary injected particles at the source we consider, additionally to protons, four classes of primary nuclei, namely Helium, CNO group, MgAlSi group and Iron. In the computation of the observed flux generated by a given primary  $A_0$  we include also all secondaries produced by the propagation. The flux of all secondaries will be presented in figures as gray shadowed regions, while the total flux generated by a given primary  $A_0$  will be presented as continuous colored lines.

The first important point to make here is that for a homogeneous distribution of sources, in order to accommodate a heavy mass composition at high energy as inferred by Auger, one is forced to require very hard injection spectra ( $\gamma_g \leq 1.6$ ) at the sources.

In Fig. 1 we illustrate this statement by showing the case  $\gamma_g = 2$ . Any steeper injection spectrum makes the contradiction even more severe (see for instance Fig. 5 of Ref. [40] and Fig. 4c of Ref. [8] and references therein).

This difficulty may be described in the following way. The low energy tail of UHECR spectra reproduces the injection spectrum  $n \propto E^{-\gamma_g}$ , as follows from the solution to the kinetic equation, Eq. (2.11). Therefore, steep injection spectra ( $\gamma_g \geq 2$ ) cause the low energy spectra ( $E \gtrsim 10^{18}$  eV) to be polluted with heavy nuclei, thereby leading to a disagreement with the light composition observed by Auger in the same energy region. This result is independent of the choice of the maximum energy.

A hard injection spectrum alleviates this problem. In Fig. 2 we plot the spectrum of individual nuclear species as calculated with the kinetic equation approach illustrated above,



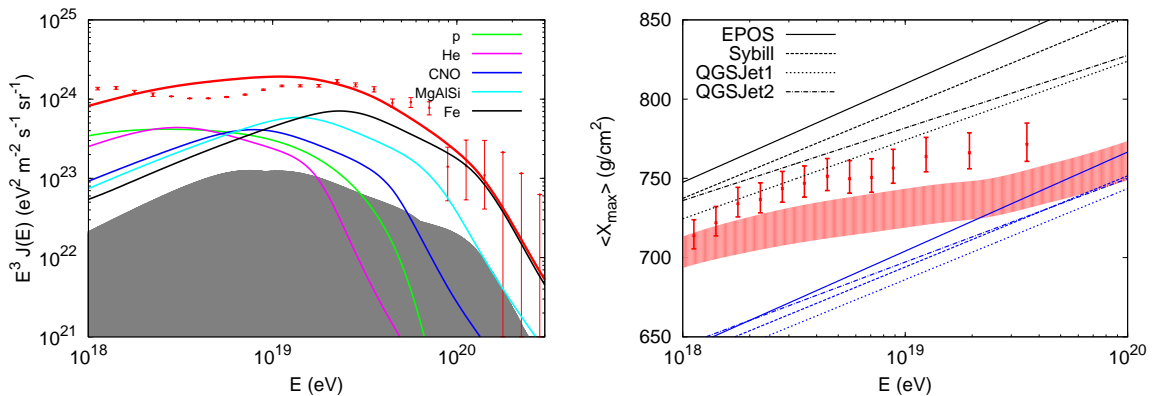


**Figure 1.** [Left panel] Fluxes of protons and nuclei in the case of an injection power law index  $\gamma_g = 2$  with primary injected particles as labelled. Curves with different colors show the sum of the flux of primaries with given mass number  $A_0$  and all secondaries produced by the same nuclear species. The thick red line shows the total spectrum. The shadowed area shows the flux of all secondaries alone. Experimental data are the Auger data on flux [38, 39]. [Right panel] Mean value of the depth of shower maximum  $\langle X_{max} \rangle$  as measured by Auger [15] and in our calculations (as in the left panel).

for  $\gamma_g = 1$ . Again, four classes of primary nuclei (helium, CNO group, MgAlSi group and Iron) are included (in addition to protons).

The fit to the Auger data is obtained by using a source emissivity  $\mathcal{L}_0 = 2 \times 10^{44}$  erg/Mpc<sup>3</sup>/y (above  $10^7$  GeV/n) and the following fractions of injection rates relative to proton injection:

$$Q_{He}^{acc} = 0.2Q_p^{acc}, \quad Q_{CNO}^{acc} = 0.06Q_p^{acc}, \quad Q_{MgAlSi}^{acc} = 0.03Q_p^{acc}, \quad Q_{Fe}^{acc} = 0.01Q_p^{acc}. \quad (3.1)$$

In Fig. 2 we used the same color codes as in Fig. 1, the maximum acceleration energy for protons is  $E_{max}^p = 5 \times 10^{18}$  eV and for nuclei  $E_{max}^A = Z \times E_{max}^p$ .

The hard injection spectra required to fit the Auger data are reminiscent of models of the origin of UHECRs associated to acceleration in rapidly rotating neutron stars [41, 42, 43, 44], although hard spectra are a more general characteristic of acceleration scenarios where regular electric fields are available (e.g. unipolar induction and reconnection).

The mean depth of shower maximum  $\langle X_{max} \rangle$  (left panel) and its dispersion (right panel) are shown in Fig. 3 for the same fluxes as reported in Fig. 2. The combination of hard injection spectrum and low  $E_{max}$  allows us to reach a satisfactory simultaneous agreement with both the spectrum at  $E > 5 \times 10^{18}$  eV and the chemical composition, though with a slight tendency toward a too heavy composition at the highest energies, thereby confirming a result previously presented in Refs. [8, 44].

The fact that a simultaneous fit to the Auger data on the spectrum at  $E > 5 \times 10^{18}$  eV and the chemical composition requires flat injection spectra with  $\gamma_g \leq 1.5 - 1.6$  also implies that the spectrum at  $E < 5 \times 10^{18}$  eV cannot be fitted in the same way, as clearly visible in Fig. 2: some kind of new component in the EeV energy region is required. Hereafter we will refer to this component as the '*additional EeV component*'. It is clear that the behavior and chemical composition of this component may have profound implications for models of the transition from Galactic to extragalactic CRs.

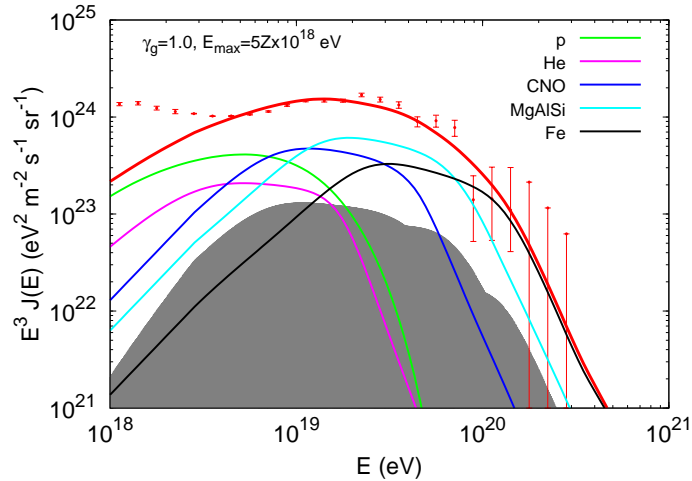


**Figure 2.** Fluxes of protons and nuclei in the case of an injection power law index  $\gamma_g = 1$  with primary injected particles as labelled. Curves with different colors show the sum of the flux of primaries with given mass number  $A_0$  and all secondaries produced by the same nuclear species. The shadowed area shows the flux of all secondaries alone. Experimental data are the Auger data on flux [38, 39].

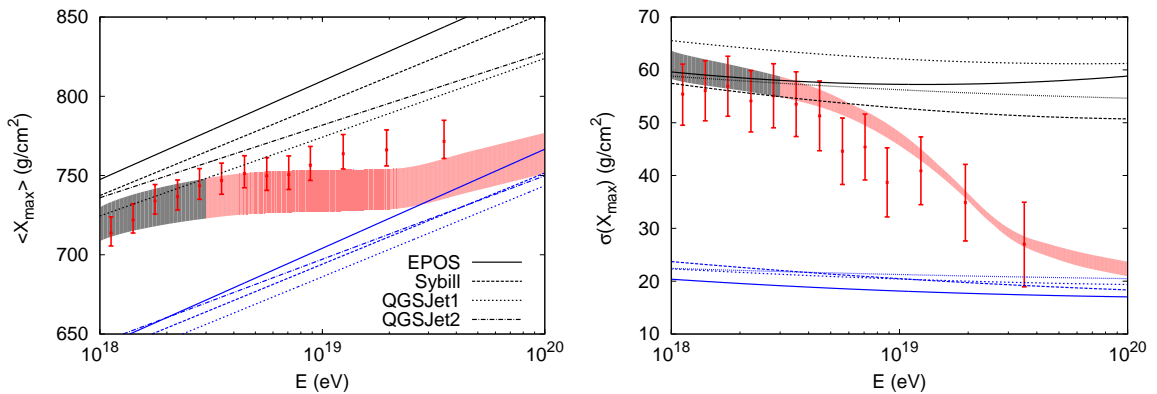


**Figure 3.** Mean value of the depth of shower maximum  $\langle X_{max} \rangle$  and its dispersion  $\sigma(X_{max})$  as measured by Auger [15] and in our calculations with the same choice of parameters as in figure 2. The gray region corresponds to the energy range in which the Auger flux is not reproduced.

Below we consider two possibilities to describe the Auger all-particle CR spectrum and chemical composition, namely the case in which the additional EeV component has a galactic origin, extending to very high energies, and the case in which the additional EeV component composed by protons and helium nuclei has an extragalactic origin.

### 3.1 Galactic EeV component

The basic version of the SNR paradigm suggests that SNRs may accelerate CRs at the SN blast wave up to rigidity  $R \sim (3 - 5) \times 10^6$  GV, which leads to iron nuclei with maximum energy  $7.8 \times 10^{16} - 1.3 \times 10^{17}$  eV. This range of energies should also correspond to the end of Galactic CRs. On the other hand it has been speculated that some rare but more energetic SN events may give rise to CRs with even larger energies [45], although there may be severe theoretical difficulties in understanding how to achieve such high energies [46].

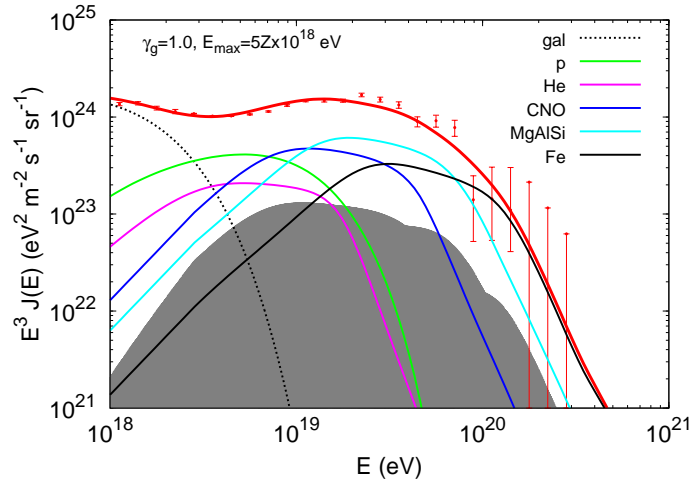


**Figure 4.** Fluxes of protons and nuclei obtained as in figure 2. The additional galactic component is plotted as dotted black line. Experimental data are the Auger data on flux [38, 39].

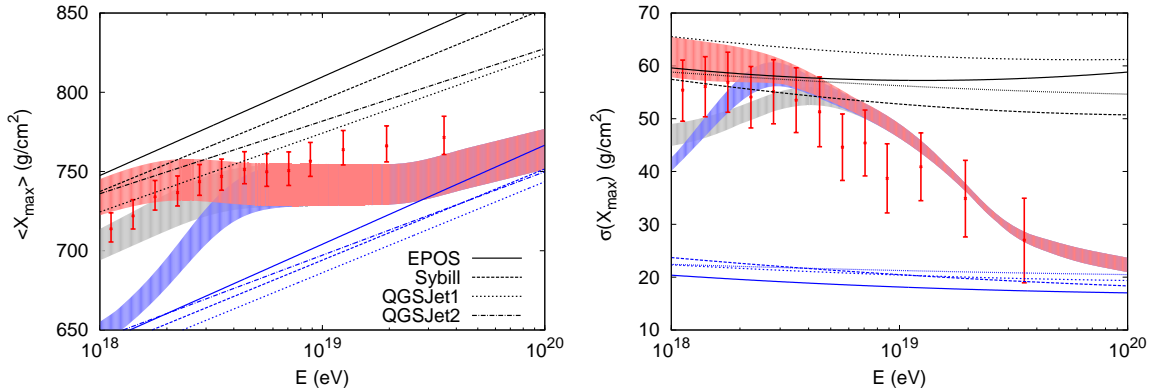


**Figure 5.** Mean value of the depth of shower maximum  $\langle X_{max} \rangle$  and its dispersion  $\sigma(X_{max})$  as measured by Auger [15] and in our calculations with the same choice of parameters of figure 4. The different colors of the shadowed regions correspond to the three choices for the additional galactic component: protons (red), helium (gray) and iron (blu).

On the other hand, as discussed above, an additional CR component appears to be required by the Auger data in the energy range  $E < 5 \times 10^{18}$  eV, therefore here we introduce such a component in the form of a speculative Galactic CR flux, parametrized as:

$$J_{gal}(E) = J_0 e^{-E/E_\star} \left( \frac{E}{E_\star} \right)^{-\gamma} \quad (3.2)$$

with  $E_\star = 10^{18}$  eV,  $\gamma = 2.65$  and  $J_0$  chosen in order to fit the observations. The choice of the power law index  $\gamma$  in equation (3.2) comes from the galactic cosmic rays spectra as computed in [47]. In figure 4 we plot the all particle spectrum with the same choice of the injection parameters used in figure 2 and the additional galactic component, Eq. (3.2), plotted as a dotted black curve.

Given the speculative nature of the Galactic component used here, we left its chemical

composition free, so as to infer it from the data. More specifically, we consider three possibilities, namely that the Galactic component consists of protons, helium or iron nuclei. The corresponding  $\langle X_{max} \rangle$  and  $\sigma(X_{max})$  are plotted in Fig. 5, where the pure proton composition is shown as a red shadowed area, the pure helium composition is shown as a gray shadowed area and, finally, the pure iron composition of the galactic component is shown as a blue shadowed area. The latter case would be favored, as far as particle acceleration is concerned [45].

The composition data shown in Fig. 5 strongly favor a proton composition or a mixture of protons and helium, but this chemical composition is excluded by the Auger data on anisotropy [48], since protons and helium in the case discussed here have a Galactic origin. The anisotropy expected for a galactic light component extending up to energies around  $10^{18}$  eV exceeds by more than one order of magnitude the upper limit measured in [48]. The same conclusion was reached by using a MC simulation of propagation in [49].

To satisfy the observations on anisotropy one should assume a pure iron composition of the additional galactic component, but this case is strongly disfavored by  $X_{max}(E)$  as measured by Auger (see the blue shadowed area in Fig. 5). In fact we tried to leave the fraction of Fe nuclei free with respect to protons in the Galactic additional component and we found that the RMS at EeV energies as observed by Auger can be reproduced only if this fraction is of order 10% or smaller.

### 3.2 Extragalactic EeV component and KASCADE-Grande light component

An additional component of extragalactic light nuclei with a generation spectrum much steeper than the one used for heavy nuclei can be introduced making use of the recent data collected by the KG collaboration, which show the existence at sub-EeV energies of a light (p+He) component with a spectral index  $\gamma = 2.79 \pm 0.08$  [17, 18]. On the other hand, the introduction of an extragalactic component of this kind can be done only in an artificial way, since there is no theoretical guidance from known acceleration models.

To reconcile such steep spectrum with the flat spectrum needed for heavy nuclei, one has to assume the existence of two classes of sources: one that provides only light elements (p+He) with a steep injection and another one with flat injection that provides also heavy nuclei. Here we will only make the minimal assumption that, in addition to the class of sources that produce protons and nuclei with flat injection spectrum (as discussed in the section above), there is also a second class of sources that injects light nuclei (protons and helium nuclei) with a generation index  $\gamma_g = 2.7$  at high energy [11, 12, 50]. Both components are assumed to have a spectral break at Lorentz factor  $\Gamma_0 = 10^7$ , physically motivated as in Refs. [28] and [12].

In Figs. 6 (left panel) and 7 we plot the fluxes and chemical composition ( $X_{max}$  and its dispersion) as obtained with these two classes of sources. We assumed a source emissivity of the light component (p+He)  $\mathcal{L}_0(p, He) = 7 \times 10^{49}$  erg/Mpc<sup>3</sup>/yr (above  $10^7$  GeV/n), with a maximum acceleration energy  $E_{max} = 3Z \times 10^{19}$  eV and an injection ratio  $Q_{He}^{acc} = 0.1Q_p^{acc}$ . The second component, contributing p, He, CNO, MgAlSi and Fe, is the same as discussed in the previous section with a slightly reduced emissivity  $\mathcal{L}_0 = 1.5 \times 10^{44}$  erg/Mpc<sup>3</sup>/yr (above  $10^7$  GeV/n) and almost the same ratios of injection rates as before (see Eq. (3.1)). The total fluxes of p and He are plotted as thick continuous green and magenta lines respectively, obtained as the sum of the two contributions to p and He spectra from the two classes of sources considered. At EeV energies sources providing also heavy nuclei give a very small contribution to the flux of p and He, as shown in Fig. 2, in this energy range the flux of light

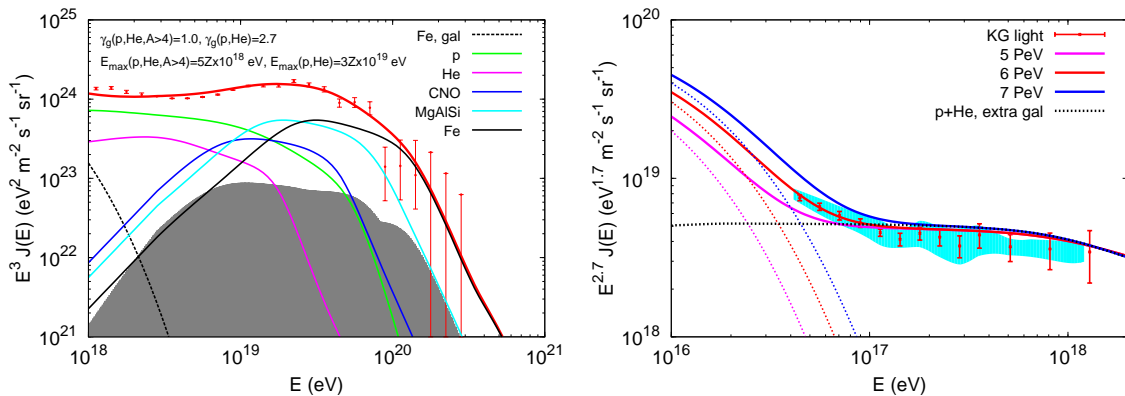


**Figure 6.** [Left panel] Fluxes of protons and nuclei in the case of two populations of extragalactic sources with an injection parameters  $\gamma_g = 2.7$ ,  $E_{max}^p = 3 \times 10^{19}$  eV for proton and helium and  $\gamma_g = 1.0$ ,  $E_{max}^p = 5 \times 10^{18}$  eV for sources providing also heavier nuclei. Curves with different colors show the sum of the flux of primaries with given mass number  $A_0$  and all secondaries produced by the same nuclear species. The shadowed area shows the flux of all secondaries alone. [Right panel] Cascade grande light component compared with extragalactic proton and helium with  $\gamma_g = 2.7$  and galactic proton and helium fluxes as computed in [47], with three different choices of the maximum acceleration energy as labeled.

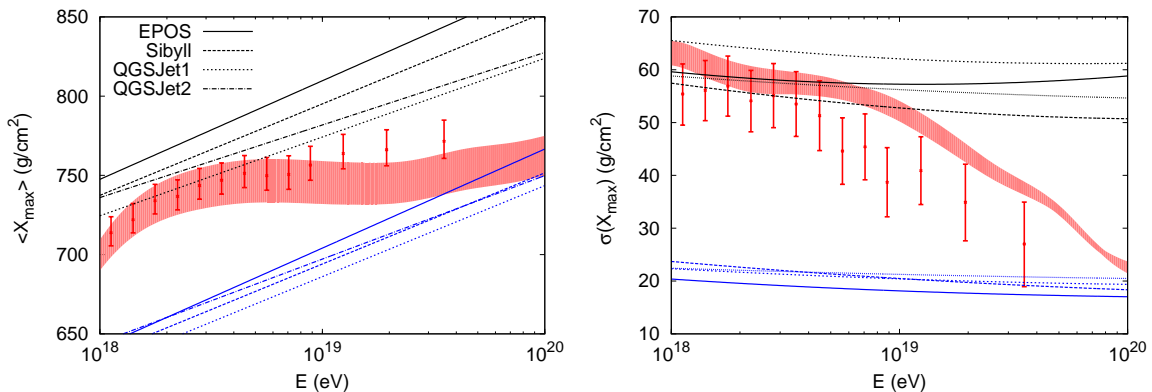


**Figure 7.** Mean value of the depth of shower maximum  $\langle X_{max} \rangle$  and its dispersion  $\sigma(X_{max})$  as measured by Auger [15] and in our calculations with the same choice of parameters as in figure 6.

elements (p+He) is contributed mainly by sources with steep injection. In the left panel of Fig. 6 the end of the proton spectrum coincides with the maximum energy reached in the sources, while the spectra of nuclei are ended by photo-disintegration on the EBL. Together with the extragalactic CR components, in the left panel of Fig. 6 we also plot the tail of the galactic (iron dominated) CR spectrum (black dotted line) as computed in Ref. [47] (with a maximum energy for galactic protons of 6 PeV, see below).

The fitting to the Auger data on spectrum and mass composition leads to conclude that at the energy of the ankle,  $\sim 5$  EeV, the flux is dominated by extragalactic CRs, thereby locating the transition from the Galactic to the extragalactic component in the range  $10^{16} - 10^{18}$  eV, with a steep light extragalactic component kicking in around  $\lesssim 10^{18}$  eV.

As anticipated above, it is interesting to notice that a light CR component has been

recently measured by the KASCADE-Grande collaboration [17, 18] and attributed to extragalactic sources. This component is claimed to match the Galactic light CR spectrum around  $10^{17}$  eV. Its spectrum, as measured by KG, has a slope  $\gamma = 2.79 \pm 0.08$ , compatible with the one inferred from our calculations based upon fitting the Auger data. The data points of KG on the light component are shown in the right panel of Fig. 6, where the shaded area illustrates the systematic uncertainties, as estimated by the collaboration. The rapidly falling dotted lines show the Galactic p+He spectrum as computed in [47], with a maximum energy of protons of 5, 6 and 7 PeV (see labels). The roughly constant black dotted line shows the flux of extragalactic light CRs as calculated above, based on the fit to the Auger data. The solid lines indicate the sum of the Galactic and extra galactic light components, showing a remarkable agreement with the KG data. It is however to be kept in mind that the values of the maximum proton energies used here are sizeably higher than the standard 3 PeV, and considerably higher than it is easy to obtain from theories of CR acceleration at SNR shocks (see for instance [46, 51]).

Here we do not want to over-interpret the KG data, since the fluxes and inferred mass composition are strongly dependent upon the adopted model for the development of showers in the atmosphere [21]. We only notice that the existence of a light component that we postulated in fitting Auger data appears naturally in the KG data.

## 4 Discussion and conclusions

In this paper we took the Auger data on the spectrum and chemical composition of UHECRs at face value and tried to infer as much physical information as possible.

The evidence that CRs in the energy region  $(1 - 5) \times 10^{18}$  eV are dominated by light elements may be considered rather solid as it follows from data on  $\langle X_{max} \rangle$  and its dispersion for the three largest UHECR detectors, Auger [15], TA [52, 53] and HiRes [54, 55]. Most of the debate on mass composition concentrates upon data at energies  $\gtrsim 5 \times 10^{18}$  eV.

Here we showed that the spectrum and mass composition of UHECRs as measured by Auger require a hard injection spectrum at the sources, with slope  $\gamma_g \leq 1.5 - 1.6$ , as also discussed in Ref. [56]. Moreover, we find that the maximum energy of nuclei with charge  $Z$  must be relatively low,  $\sim 5 \times 10^{18} Z$  eV. One should appreciate the change of paradigm that is taking place in the aftermath of the Auger data: in the last decade we moved from a need to accelerate protons up to energies in excess of  $10^{20}$  eV to the requirement to limit the maximum energy of protons to  $\lesssim 5$  EeV.

From the theoretical point of view the hard injection spectrum is interesting in that it suggests that acceleration mechanisms such as those that take place in the magnetosphere of rapidly rotating neutron stars [41, 42, 43, 44] or in the accretion discs around massive black holes [57] may play a role. Moreover, it is fair to assume that the environment around a neutron star may be polluted with heavy nuclei, provided such nuclei can be stripped off the surface of the star. Propagation of these nuclei in the expanding ejecta of the parent SN is expected to produce lighter elements because of spallation and photo-disintegration. As a result, a mixed composition is expected when CRs escape the source environment [43, 44].

The most disappointing consequence of the hard injection spectra is that the Auger spectrum can only be fitted for energies  $\gtrsim 5 \times 10^{18}$  eV, while lower energy CRs require a different explanation. Filling this gap requires the introduction of an *ad hoc* CR component and we showed here that such component must be composed of extragalactic light nuclei (p+He) with an injection spectrum with slope  $\sim 2.7$ . The most straightforward implication

of this fact is that the transition from Galactic to extragalactic CRs must be taking place at energies  $\lesssim 10^{18}$  eV rather than at the ankle.

One could be tempted to speculate that the necessary extra component may be provided by Galactic sources, able to accelerate particles to much higher maximum energies. If these CRs were heavy nuclei, the mass composition in the energy region 1 – 5 EeV would not be in agreement with the  $X_{max}$  and dispersion as observed by Auger (as well as by HiRes and TA). On the other hand, a light composition of Galactic CRs at such high energies would conflict with our common wisdom of particle acceleration in SNRs: even in models involving energetic, rare SN events [45] the maximum energy may reach  $\sim 10^{18}$  eV but only for iron nuclei and with rather extreme assumptions. Even if the maximum energy were high enough, the predicted anisotropy would be wildly in excess of observations [48]. The fair conclusion is to deduce that the extra component must be made of extragalactic light nuclei (p+He), as discussed above.

Remarkably this light component has a spectrum and flux which are compatible with the recently detected flux of light nuclei in the energy region  $10^{16} - 10^{18}$  eV by KASCADE-Grande [18]. These data show an ankle-like feature at  $\sim 10^{17}$  eV, that may be tentatively associated to the transition to extragalactic protons.

The disappointing complexity of the viable explanations for the spectrum and chemical composition of Auger are probably the sign that the injection spectra needed to fit the data are themselves the result of a more complex phenomenology. An instance of this could be the propagation in extragalactic magnetic fields [40, 58, 59, 60] and/or phenomena that occur inside the sources that may also potentially affect the spectra of nuclei injected on cosmological scales and possibly preferentially select high energy nuclei.

## Acknowledgments

We are grateful to the rest of the Arcetri High Energy Astrophysics Group and to the Auger group of L'Aquila University for continuous discussions on the subject of UHECR. We also thank K.H. Kampert for valuable discussions on the KASCADE-Grande data. We also thank the anonymous referee that helped us improving the paper.

## References

- [1] V. Ptuskin, *Propagation of galactic cosmic rays*, *Astropart.Phys.* **39-40** (2012) 44–51.
- [2] P. Blasi, *The origin of galactic cosmic rays*, *The Astronomy and Astrophysics Review* **21** (Nov, 2013) 70. (c) 2013: Springer-Verlag Berlin Heidelberg.
- [3] R. Blandford and D. Eichler, *Particle acceleration at astrophysical shocks: A theory of cosmic ray origin*, *Physics Reports* **154** (Oct, 1987) 1.
- [4] M. A. Malkov and L. O. Drury, *Nonlinear theory of diffusive acceleration of particles by shock waves*, *Reports on Progress in Physics* **64** (Apr, 2001) 429.
- [5] D. Caprioli, E. Amato, and P. Blasi, *The contribution of supernova remnants to the galactic cosmic ray spectrum*, *Astroparticle Physics* **33** (Apr, 2010) 160–168.
- [6] F. W. Stecker, M. Malkan, and S. Scully, *Intergalactic photon spectra from the far ir to the uv lyman limit for  $0 < z < 6$  and the optical depth of the universe to high energy gamma-rays*, *Astrophys.J.* **648** (2006) 774–783, [[astro-ph/0510449](https://arxiv.org/abs/astro-ph/0510449)].

- [7] T. M. Kneiske, T. Bretz, K. Mannheim, and D. Hartmann, *Implications of cosmological gamma-ray absorption. 2. Modification of gamma-ray spectra*, *Astron.Astrophys.* **413** (2004) 807–815, [[astro-ph/0309141](#)].
- [8] D. Allard, *Extragalactic propagation of ultrahigh energy cosmic-rays*, *Astropart.Phys.* **39-40** (2012) 33–43, [[arXiv:1111.3290](#)].
- [9] R. Aloisio, V. Berezhinsky, and S. Grigorieva, *Analytic calculations of the spectra of ultra-high energy cosmic ray nuclei. I. The case of CMB radiation*, *Astropart.Phys.* **41** (2013) 73–93, [[arXiv:0802.4452](#)].
- [10] R. Aloisio, V. Berezhinsky, and S. Grigorieva, *Analytic calculations of the spectra of ultra high energy cosmic ray nuclei. II. The general case of background radiation*, *Astropart.Phys.* **41** (2013) 94–107, [[arXiv:1006.2484](#)].
- [11] V. Berezhinsky, A. Gazizov, and S. Grigorieva, *On astrophysical solution to ultrahigh-energy cosmic rays*, *Phys.Rev.* **D74** (2006) 043005, [[hep-ph/0204357](#)].
- [12] R. Aloisio, V. Berezhinsky, P. Blasi, A. Gazizov, S. Grigorieva, and B. Hnatyk, *A dip in the UHECR spectrum and the transition from galactic to extragalactic cosmic rays*, *Astropart.Phys.* **27** (2007) 76–91, [[astro-ph/0608219](#)].
- [13] K. Greisen, *End to the cosmic ray spectrum?*, *Phys.Rev.Lett.* **16** (1966) 748–750.
- [14] G. Zatsepin and V. Kuzmin, *Upper limit of the spectrum of cosmic rays*, *JETP Lett.* **4** (1966) 78–80.
- [15] **Pierre Auger Collaboration**, J. Abraham *et. al.*, *Measurement of the Depth of Maximum of Extensive Air Showers above  $10^{18}$  eV*, *Phys.Rev.Lett.* **104** (2010) 091101, [[arXiv:1002.0699](#)].
- [16] E. Barcikowski, J. Bellido, J. Belz, Y. Egorov, S. Knurenko, V. de Souza, Y. Tameda, Y. Tsunesada, M. U. for the Pierre Auger, T. Array, and Y. Collaborations, *Mass composition working group report at uhecr-2012*, *arXiv astro-ph.HE* (Jun, 2013) [[arXiv:1306.4430](#)].
- [17] **KASCADE-Grande Collaboration** Collaboration, W. Apel *et. al.*, *Kneelike structure in the spectrum of the heavy component of cosmic rays observed with KASCADE-Grande*, *Phys.Rev.Lett.* **107** (2011) 171104, [[arXiv:1107.5885](#)].
- [18] W. Apel, J. Arteaga-Velázquez, K. Bekk, M. Bertaina, J. Blmer, *et. al.*, *Ankle-like Feature in the Energy Spectrum of Light Elements of Cosmic Rays Observed with KASCADE-Grande*, *Phys.Rev.* **D87** (2013) 081101, [[arXiv:1304.7114](#)].
- [19] M. G. A. *et al.* (ICETOP Coll.), *Measurement of the cosmic ray energy spectrum with icetop-73*, *Phys. Rev.* **88** (2013), no. D88 042004.
- [20] K.-H. Kampert, *Ultra-High Energy Cosmic Rays: Results and Prospects*, *ArXiv e-prints* (May, 2013) [[arXiv:1305.2363](#)].
- [21] W. D. Apel, J. C. Arteaga-Velázquez, K. Bekk, M. Bertaina, J. Blümer, H. Bozdog, I. M. Brancus, E. Cantoni, A. Chiavassa, F. Cossavella, K. Daumiller, V. de Souza, F. D. Pierro, P. Doll, R. Engel, J. Engler, M. Finger, B. Fuchs, D. Fuhrmann, H. J. Gils, R. Glasstetter, C. Grupen, A. Haungs, D. Heck, J. R. Hörandel, D. Huber, T. Huege, K.-H. Kampert, D. Kang, H. O. Klages, K. Link, P. uczak, M. Ludwig, H. J. Mathes, H. J. Mayer, M. Melissas, J. Milke, B. Mitrica, C. Morello, J. Oehlschläger, S. Ostapchenko, N. Palmieri, M. Petcu, T. Pierog, H. Rebel, M. Roth, H. Schieler, S. Schoo, F. G. Schröder, O. Sima, G. Toma, G. C. Trinchero, H. Ulrich, A. Weindl, J. Wochele, M. Wommer, and J. Zabierowski, *The cascade-grande energy spectrum of cosmic rays and the role of hadronic interaction models*, *ADVANCES IN SPACE RESEARCH* **53** (May, 2014) 1456.
- [22] R. Aloisio, D. Boncioli, A. Grillo, S. Petrera, and F. Salamida, *SimProp: a Simulation Code for Ultra High Energy Cosmic Ray Propagation*, *JCAP* **1210** (2012) 007, [[arXiv:1204.2970](#)].



- [23] D. Allard, E. Parizot, E. Khan, S. Goriely, and A. Olinto, *UHE nuclei propagation and the interpretation of the ankle in the cosmic-ray spectrum*, *Astron.Astrophys.* **443** (2005) L29–L32, [[astro-ph/0505566](#)].
- [24] E. Armengaud, G. Sigl, T. Beau, and F. Miniati, *Crpropa: a numerical tool for the propagation of uhe cosmic rays, gamma-rays and neutrinos*, *Astropart.Phys.* **28** (2007) 463–471, [[astro-ph/0603675](#)].
- [25] F. Stecker and M. Salamon, *Photodisintegration of ultrahigh-energy cosmic rays: A New determination*, *Astrophys.J.* **512** (1999) 521–526, [[astro-ph/9808110](#)].
- [26] J. Puget, F. Stecker, and J. Bredekamp, *Photonuclear Interactions of Ultrahigh-Energy Cosmic Rays and their Astrophysical Consequences*, *Astrophys.J.* **205** (1976) 638–654.
- [27] N. Gerasimova and I. Rozental, *Interaction of Nuclei and Photons of High Energies with a Thermal Radiations in the Universe*, *JETP* **41** (1961) 488.
- [28] M. Kachelriess and D. V. Semikoz, *Reconciling the ultra-high energy cosmic ray spectrum with Fermi shock acceleration*, *Phys.Lett.* **B634** (2006) 143–147, [[astro-ph/0510188](#)].
- [29] V. Berezhinsky and S. Grigor’eva, *A Bump in the ultrahigh-energy cosmic ray spectrum*, *Astron.Astrophys.* **199** (1988) 1–12.
- [30] R. Aloisio, V. Berezhinsky, P. Blasi, and S. Ostapchenko, *Signatures of the transition from Galactic to extragalactic cosmic rays*, *Phys.Rev.* **D77** (2008) 025007, [[arXiv:0706.2834](#)].
- [31] K.-H. Kampert and M. Unger, *Measurements of the Cosmic Ray Composition with Air Shower Experiments*, *Astropart.Phys.* **35** (2012) 660–678, [[arXiv:1201.0018](#)].
- [32] R. Engel, D. Heck, and T. Pierog, *Extensive air showers and hadronic interactions at high energy*, *Ann.Rev.Nucl.Part.Sci.* **61** (2011) 467–489.
- [33] **Pierre Auger Collaboration** Collaboration, P. Abreu *et. al.*, *Interpretation of the Depths of Maximum of Extensive Air Showers Measured by the Pierre Auger Observatory*, *JCAP* **1302** (2013) 026, [[arXiv:1301.6637](#)].
- [34] T. Pierog and K. Werner, *Muon Production in Extended Air Shower Simulations*, *Phys.Rev.Lett.* **101** (2008) 171101, [[astro-ph/0611311](#)].
- [35] E.-J. Ahn, R. Engel, T. K. Gaisser, P. Lipari, and T. Stanev, *Cosmic ray interaction event generator SIBYLL 2.1*, *Phys.Rev.* **D80** (2009) 094003, [[arXiv:0906.4113](#)].
- [36] N. Kalmykov, S. Ostapchenko, and A. Pavlov, *Quark-gluon string model and EAS simulation problems at ultra-high energies*, *Nucl.Phys.Proc.Suppl.* **52B** (1997) 17–28.
- [37] S. Ostapchenko, *Non-linear screening effects in high energy hadronic interactions*, *Phys.Rev.* **D74** (2006) 014026, [[hep-ph/0505259](#)].
- [38] **Pierre Auger** Collaboration, P. Abreu *et. al.*, *The Pierre Auger Observatory I: The Cosmic Ray Energy Spectrum and Related Measurements*, [[arXiv:1107.4809](#)].
- [39] **Pierre Auger** Collaboration, F. Salamida, *Update on the measurement of the CR energy spectrum above  $10^{18}$ -eV made using the Pierre Auger Observatory*, .
- [40] R. Aloisio, V. Berezhinsky, and A. Gazizov, *Ultra High Energy Cosmic Rays: The disappointing model*, *Astropart.Phys.* **34** (2011) 620–626, [[arXiv:0907.5194](#)].
- [41] P. Blasi, R. I. Epstein, and A. V. Olinto, *Ultrahigh-energy cosmic rays from young neutron star winds*, *Astrophys.J.* **533** (2000) L123, [[astro-ph/9912240](#)].
- [42] J. Arons, *Magnetars in the metagalaxy: an origin for ultrahigh-energy cosmic rays in the nearby universe*, *Astrophys.J.* **589** (2003) 871–892, [[astro-ph/0208444](#)].
- [43] K. Fang, K. Kotera, and A. V. Olinto, *Newly-born pulsars as sources of ultrahigh energy cosmic rays*, *Astrophys.J.* **750** (2012) 118, [[arXiv:1201.5197](#)].

- [44] K. Fang, K. Kotera, and A. V. Olinto, *Ultrahigh Energy Cosmic Ray Nuclei from Extragalactic Pulsars and the effect of their Galactic counterparts*, *JCAP* **1303** (2013) 010, [[arXiv:1302.4482](#)].
- [45] V. Ptuskin, V. Zirakashvili, and E.-S. Seo, *Spectrum of Galactic Cosmic Rays Accelerated in Supernova Remnants*, *ApJ* **718** (2010) 31.
- [46] K. M. Schure and A. R. Bell, *Cosmic ray acceleration in young supernova remnants*, *MNRAS* (Aug., 2013) [[arXiv:1307.6575](#)].
- [47] R. Aloisio and P. Blasi, *Propagation of galactic cosmic rays in the presence of self-generated turbulence*, *JCAP* **1307** (2013) 001, [[arXiv:1306.2018](#)].
- [48] Pierre Auger Collaboration, P. Abreu, M. Aglietta, M. Ahlers, E. J. Ahn, I. F. M. Albuquerque, D. Allard, I. Allekotte, J. Allen, P. Allison, and et al., *Constraints on the Origin of Cosmic Rays above  $10^{18}$  eV from Large-scale Anisotropy Searches in Data of the Pierre Auger Observatory*, *ApJ* **762** (Jan., 2013) L13, [[arXiv:1212.3083](#)].
- [49] G. Giacinti, M. Kachelrieß, D. V. Semikoz, and G. Sigl, *Cosmic ray anisotropy as signature for the transition from galactic to extragalactic cosmic rays*, *JCAP* **7** (July, 2012) 31, [[arXiv:1112.5599](#)].
- [50] R. Aloisio, V. Berezhinsky, and A. Gazizov, *Transition from galactic to extragalactic cosmic rays*, *Astropart.Phys.* **39-40** (2012) 129–143, [[arXiv:1211.0494](#)].
- [51] P. Blasi, *Origin of very high and ultra high energy cosmic rays*, eprint *arXiv* **1403** (Mar, 2014) 2967.
- [52] **Telescope Array** Collaboration, C. C. Jui, *Cosmic Ray in the Northern Hemisphere: Results from the Telescope Array Experiment*, *J.Phys.Conf.Ser.* **404** (2012) 012037, [[arXiv:1110.0133](#)].
- [53] **Telescope Array** Collaboration, Y. Tsunesada, *Highlights from Telescope Array*, [arXiv:1111.2507](#).
- [54] **High Resolution Fly’s Eye** Collaboration, R. Abbasi et. al., *Measurement of the flux of ultrahigh energy cosmic rays from monocular observations by the High Resolution Fly’s Eye experiment*, *Phys.Rev.Lett.* **92** (2004) 151101, [[astro-ph/0208243](#)].
- [55] **HiRes** Collaboration, R. Abbasi et. al., *First observation of the Greisen-Zatsepin-Kuzmin suppression*, *Phys.Rev.Lett.* **100** (2008) 101101, [[astro-ph/0703099](#)].
- [56] A. M. Taylor, *UHECR composition models*, *Astroparticle Physics* **54** (Feb., 2014) 48–53, [[arXiv:1401.0199](#)].
- [57] R. D. Blandford, *Accretion disc electrodynamics - A model for double radio sources*, *MNRAS* **176** (1976) 465–481.
- [58] R. Aloisio and V. Berezhinsky, *Anti-GZK effect in UHECR diffusive propagation*, *Astrophys.J.* **625** (2005) 249–255, [[astro-ph/0412578](#)].
- [59] M. Lemoine, *Extra-galactic magnetic fields and the second knee in the cosmic-ray spectrum*, *Phys.Rev.* **D71** (2005) 083007, [[astro-ph/0411173](#)].
- [60] S. Mollerach and E. Roulet, *Magnetic diffusion effects on the Ultra-High Energy Cosmic Ray spectrum and composition*, [arXiv:1305.6519](#).